Windiness spells in SW Europe since the Last Glacial Maximum

Susana Costas[*,1, 2], Filipa Naughton[3], Ronald Goble[4] and Hans Renssen[5]

[*] *Corresponding author: scotero@ualg.pt*

[1]*Current address. Centro de Investigação Marinha e Ambiental, Universidade do Algarve, Portugal*

[2]*Laboratório Nacional de Energia e Geologia, Portugal*

[3]*Instituto Português do Mar e da Atmosfera, Portugal*

[4]*Department of Earth and Atmospheric Sciences, University of Nebraska, Lincoln, USA*

[5]*Department of Earth Sciences, Vrije Universiteit Amsterdam, The Netherlands*

ABSTRACT

Dunefields have a great potential to unravel past regimes of atmospheric circulation as they record direct traces of this component of the climate system. Along the Portuguese coast, transgressive dunefields represent relict features originated by intense and frequent westerly winds that largely contrast with present conditions, clearly dominated by weaker northwesterly winds. Optical dating and subsurface stratigraphy document three age clusters indicating main episodes of dune mobilization during: the last termination (20-11.6 ka), Middle Holocene (5.6 ka), and Late Holocene (1.2-0.98 and 0.4-0.15 ka).

We find reconstructed windfields to be analogous during all episodes and dominated by strong westerlies. Yet, larger grain size diameters and dune volumes documented for the last termination support amplified patterns compatible with a southward shift and intensification of the North Atlantic westerlies during winters.

Conversely, dunes deposited after the Middle Holocene are compatible with more variable windfields and weakened patterns controlled by interannual shifts towards low values of the North Atlantic Oscillation (NAO).

This work demonstrates that present windfield regimes in southern Europe are not compatible with past aeolian activity. Indeed, present day analogs indicate that wind intensities compatible with past aeolian activity are rare at present (sediment transport potentials below estimates in the aeolian record), but can occur if the jet stream is diverted to the south (i.e. 30ºN with negative NAO index) or if very deep cyclones anchor around 50ºN, extending their influence to the western Portuguese coast (relatively low NAO index). However, these conditions represent temporary patterns lasting around one day, while we suggest that the identified episodes of aeolian activity may represent semi-permanent conditions.

1. INTRODUCTION

The Mediterranean region has become a zone of major scientific interest in the context of future climate change as projections anticipate increasing risks of droughts and problems with water availability (Seager et al., 2014). In response to this more and more urgent concern and to better anticipate ensuing consequences, a considerable effort is being devoted to understand the mechanisms governing climate variability in this region under present (Ulbrich et al., 2012) and past climatic conditions (Beghin et al., 2015). Proxy records of past conditions are essential to extend available instrumental datasets, which due to their limited lengths are not able to capture the whole variability of the climate system. Additionally, proxy records are also important to evaluate numerical climate models, which may also be used for projections of future climate. However, recent works have found conflicting evidence when attempting to explain past climate regimes based on present atmospheric circulation patterns (Dawson et al., 2002; Sorrel et al., 2012; Trouet et al., 2012).

Disparities between proxy-based signals and modeling simulations may derive from (i) unsolved uncertainties within climate variability, which are often related to the unknown past characteristics of the major modes of atmospheric circulation, such as the North Atlantic Oscillation (NAO), and (ii) inconsistencies between different proxies related to the ambiguous character of signals captured by indicators. Within this context, the need for well-resolved palaeoenvironmental records has become more and more important.

Dune deposits have a great potential as windfield regime indicators as they record essential characteristics of this element of the climate system during their formation. In turn, the state of the NAO, the major of atmospheric circulation within the North Atlantic (NA), is characterized by an index, which is often interpreted as an indicator of the strength of the westerlies over the eastern NA. Traditionally, dune deposits have been attributed to drier or colder climates contributing to vegetation decline and thus enhanced aeolian mobility (Lancaster, 1981). However, new and improved records suggest stronger links to wind strength proxies (Chase, 2009). Additionally, it is widely accepted that dunes respond to climate variability (Tsoar, 2005), confirming their potential as paleoclimate indicators.

Within this context, Costas et al. (2012) applied optically stimulated luminescence (OSL) for age determination and ground penetrating radar (GPR) for imaging the internal architecture of a transgressive dunefield at the central coast of Portugal. The explored coast is situated at the southernmost position of the NA jet stream, which in turn explains most of the precipitation within the western Mediterranean, in particular at the Iberian Peninsula (Cortesi et al., 2014). Four phases of major aeolian activity centered at 12.6, 5.6, 1.2, and 0.4 ka were identified and associated to enhanced storminess in southern Europe (Costas et al., 2012). Additionally, a good temporal correspondence was found among aeolian activity events from northern to southern Europe, suggesting simultaneous periods of enhance storminess across Europe. These evidence were reconciled to favorable patterns of atmospheric circulation, suggesting prolonged negative phases of the NAO compatible with enhanced storminess and westerly winds in southern Europe during winter while the same conditions could be recorded during summer across northern Europe. However, if long term reconstructions of the NAO are closely observed, we cannot find periods of prolonged negative phases of the NAO as it is the case for the positive mode (Baker et al., 2015; Trouet et al., 2009). Additionally, Costas et al. (2012) assessment of past aeolian activity lacks information about the major driver of aeolian activity, i.e. wind power, leading to questions such as which are the favorable conditions to promote aeolian activity, and are these conditions compatible with the present-day wind regime? These raise the need for a deeper understanding of the mechanisms behind aeolian activity in the Portuguese coast with implications for local and regional atmospheric circulation.

This work aims to develop mechanistic scenarios of enhanced storminess impacting SW European coasts. We extend the data of Costas et al. (2012) back in time to the Last Glacial Maximum (LGM), intensively exploring the inland dunefield by providing 24 new OSL dates, and reconstructing past wind conditions and atmospheric patterns. The new dates confirm earlier conclusions suggested by Costas et al. (2012) on the earliest phases (i.e. confirmation of the YD as a phase of aeolian activity and also previous cold phases). In particular, we will focus on: (i) testing the application of modern observations of atmospheric conditions for reconstructing past conditions, (ii) understanding whether or not atmospheric conditions were similar for the different episodes of past dune formation, and (iii) seeking for consistencies with other paleoclimate records in W Europe. Finally, we will test the supportive hypothesis of a common factor driving major episodes of aeolian activity in the past.

2. STUDY AREA

This work explores a fixed transgressive dunefield located at the central coast of Portugal, south of the present Tagus ebb delta. Today, this region is characterized by relatively weak average winds of around 5 m/s. Averaged values of precipitation per year for the period between 1900 and 2000 AD was about 725 mm, with values ranging between 500 and 1000 mm (Lima et al., 2005). The latter indicates precipitation values well above the threshold needed for vegetation development.

At present, aeolian sedimentation is characterized by small scale processes allowing the formation of relatively low foredunes at the back of the beach. These foredunes are frequently eroded by wave action during severe winters and partially recovered and vegetated as weather conditions improve, leading to the formation of embrionic dunes at the base of the dune scarp. Dune scarping promotes the partial fragmentation of foredunes through small-scale blowouts, which ultimately contribute to the growth of foredune ridges that may reach 10 m above mean sea level (MSL). The coastal plain extends seaward from the toe of a 60 m-high unconsolidated cliff and is characterized by a set of four foredune ridges formed after 900 yrs ago (Costas et al., 2012).

The transgressive dunefield developed on top of a terrace located inland of the edge of the cliff, at around 60 m above mean sea level (MSL). The dunefield can be considered as perched dunes formed on top of a pre-existing geological formation, and extends up to 4.5 km inland and is 42 km^2 in areal extent (Costas et al., 2012). This dunefield includes the Caparica cliff-top dune and the inland extension of the aeolian system, the Apostiça transgressive dunefield, constituting a good example of past widespread aeolian activity along the Portuguese coast. The cliff-top dune consists of a dune ridge reaching 100 m above MSL and located immediately landward of the edge of the cliff. This dune ridge was classified as a merged dune included in the compound parabolic dunes type (Costas et al., 2012). Three different radar units were identified within the ridge and related to the inland advance of transgressive dunes after the Middle Holocene (Costas et al., 2012). The Apostiça transgressive dunefield extends 5 km inland of the cliff edge and is represented by partially-filled to filled superimposed parabolic dunes advancing eastward (Costas et al., 2012).

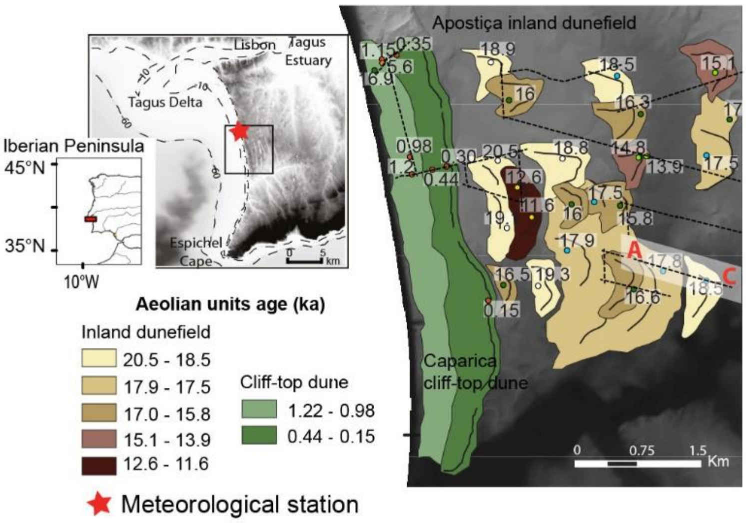

Figure 1. Location of the explored transgressive dunefield inland of the Trafaria-Espichel Cape littoral arch. The right panel shows the ages of the major aeolian units. The location of the GPR panel is pointed out with the letters A and C.

3. METHODS

Aeolian dunes provide excellent records of windfield variability through time by combining chronology and aerial photographs (Lancaster et al., 2002). In addition, dune accretion episodes can be determined if geophysical techniques are used to resolve the stratigraphy of aeolian deposits. Here, we combine new information from GPR and

OSL dates to complete and extend back in time the dataset of Costas et al. (2012) in order to reconstruct past events of aeolian activity at the Portuguese coast (Fig. 1). (For details of GPR survey and data processing see Costas et al. (2012).

Sediment sampling strategy was defined based on the results from GPR and the 10 m resolution digital terrain model of the transgressive dunefield. The spatial coverage of the samples was designed to determine the temporal distribution of the different dune building episodes. The dominance of isolated units resulting from the advance of individual parabolic dunes, rather than vertically stacked units, obliged to randomly collect the samples to account for age determination in a larger number of individual dune buildings within the inland coversand. This approach was used to avoid sampling bias limitations during the interpretation of the results in terms of age frequency and distribution supporting the reliability of the OSL accumulation chronologies and thus palaeoclimatic interpretation. A total of 22 new sediment samples were collected from the subsurface (about 1.5 m from the surface) within the transgressive dunefield while only two new samples were collected in the cliff-top dune ridge for OSL dating, textural and compositional characterization. Additionally, sediment samples from the foredune were collected and textural parameters estimated.

OSL analyses were based on the Single Aliquot Regenerative Dose (SAR) protocol (Murray and Wintle, 2000). The details of the OSL analysis and sample preparation are provided in Costas et al. (2012). All equivalent dose values (De) were determined using the Central Age Model (Galbraith et al., 1999), unless data analysis indicates partial bleaching, in which case the Minimum Age Model (Galbraith et al., 1999) was used. All ages are quoted in years before 2012.

Atmospheric circulation patterns compatible with past dune migration were evaluated and compared with local winds recorded at the present beach (Meteorological station-773, Fig. 1). The available dataset is represented by a ten year (2002 to 2012) series of local winds measured every 10 min, 10 m above ground level and provided by the Portuguese Institute for Ocean and Atmosphere. Because wind characterization may be biased by the reduced length of the available wind record, we have included a 49 year hindcast of surface winds for the Iberian Peninsula (Jerez et al., 2013; Lorente-Plazas et al., 2014). The wind dataset extracted for the study area consists of hourly winds resulting from a dynamical downscaling experiment, with a spatial resolution of 10 km, covering the Iberian Peninsula (IP), driven by the ERA40 reanalysis (1959-2001) extended by European Centre for Medium-Range Weather Forecast (ECMWF) analysis (2002-2007) (Jerez et al., 2013; Lorente-Plazas et al., 2014). Simulated winds show generally good temporal correlation with local data, but they systematically overestimate wind magnitude (Lorente-Plazas et al., 2014). Unfortunately, overestimation can be maximum for the zonal wind component in the north of the Iberian Peninsula and some of the worst correlations were observed along coastal areas (Lorente-Plazas et al., 2014). To evaluate the difference between simulated and observed local data, both datasets are compared for the overlapping period (2002-2007).

Simulated wind dataset were used to evaluate dune mobility under present-day conditions. For that, we first evaluate local windiness estimating the drift potential of the local and simulated winds to produce the associated sand roses following the methodology proposed by Fryberger (1979):

$$DP = \sum q = \frac{U^2(U - U_t)}{100} t$$

where U is the wind velocity (in knots), measured at 10 m, U_t is the threshold wind velocity (=12 knots) used in Fryberger (1979) and t is the time the wind blew above the threshold velocity (in percent). Additionally, potential sediment transport compatible with the characteristics of the transgressive dunefield was estimated applying the equation proposed by Lettau and Lettau (1977):

$$Q = K\,(\rho/g)\sqrt{D/D_{ref}}\,u_*^2(u_* - u_{*t})$$

where *K* is a surface sediment dependent constant with a value of 4.2; ρ is the air density, 1.25 kg m^{-3}; g is the acceleration due to gravity, 9.81 m s^{-2}; *D* is the median grain diameter representative of the transgressive dunes and the foredune; D_{ref} is reference median sediment grain size (0.25 mm); u_* is the shear velocity; and u_{*t} is the threshold shear velocity. Theoretic threshold wind velocities were estimated applying the Bagnold (1941) equation:

$$u_{*t} = A[gD(\rho_s - \rho)/\rho]^{1/2}$$

where u_{*t} is the threshold shear velocity; ρ_s is the density of the sediment, 2650 kg m^{-3}; and *A* is a constant of 0.085 during active saltation. Other variables such as humidity or vegetation may increase the value of the threshold shear velocity. However those are not considered on our simple approach, leading to results of thresholds below the real ones and to overestimated values of potential sediment transport.

Shear velocities can be transformed into wind speeds measured at 10 m applying the logarithmic law-of-the-wall:

$$u_z = (u_*/k)\ln(z/z_o)$$

where u_z is the wind speed at the elevation z; *k* the von Karman´s constant, i.e. 0.4 and z_o is the roughness length of the surface defined by Bagnold (1941); $z_o = D_{50}/30$, where D_{50} is the median grain size diameter.

4. RESULTS

4.1 Aeolian activity over the past

The stratigraphy and chronology of the dunefields allow us to detect discrete phases of aeolian activity separated by gaps in the overall OSL age errors distribution peaking at 0.35, 1.10, 5.60 and 17.5 ka (Table 1 Supplemental Material, Fig. 2). Time bins of 1000 years were applied to the Late-Pleistocene units (errors ranged between 600 and 1200 yrs) while Holocene units were clustered using time bins of 500 (errors ranging between 210 and 10 years). The older identified episode, which represents the encroachment of the inland coversand, was assigned to the last termination (time period between 22.0 to 11.5 ka according to Björck et al. (1998)) and represents an almost continuous event extending from 20.5 to 11.6 ka. Aeolian activity during this episode was maximum at 17.5 ka, decreased after 15.1 ka and stopped after 11.6 ka.

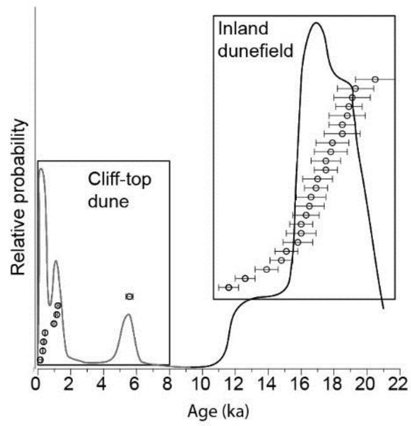

Figure 2. Relative probability plot of OSL ages. The entire dataset includes 24 OSL ages from the explored transgressive dunefield (i.e. the cliff-top dune and the inland dunefield). The peaks represent discrete phases of aeolian activity separated by gaps in the overall OSL age errors distribution. Bin sizes of 1000 years have been applied to identify last termination phases while Holocene phases were separated using 500 years bins.

Dune stratigraphy and morphology of the inland coversand indicates that dunes are spatially organized to form superimposed parabolic dunes oriented eastward (orientations between 240 and 270°). The latter suggests successive pulses of aeolian sand as supported by the obtained stratigraphy, which shows aeolian buildings formed by one unit overlaying the Pleistocene terrace (Fig. 3). Internally, units consist of several packages or subunits separated by second order surfaces, which define internal packages or sub-units interpreted as representing the migration of superimposed dunes (Fig. 3). Additionally, third order bounding surfaces within the set of cross strata indicate reactivation surfaces formed by fluctuations in airflow.

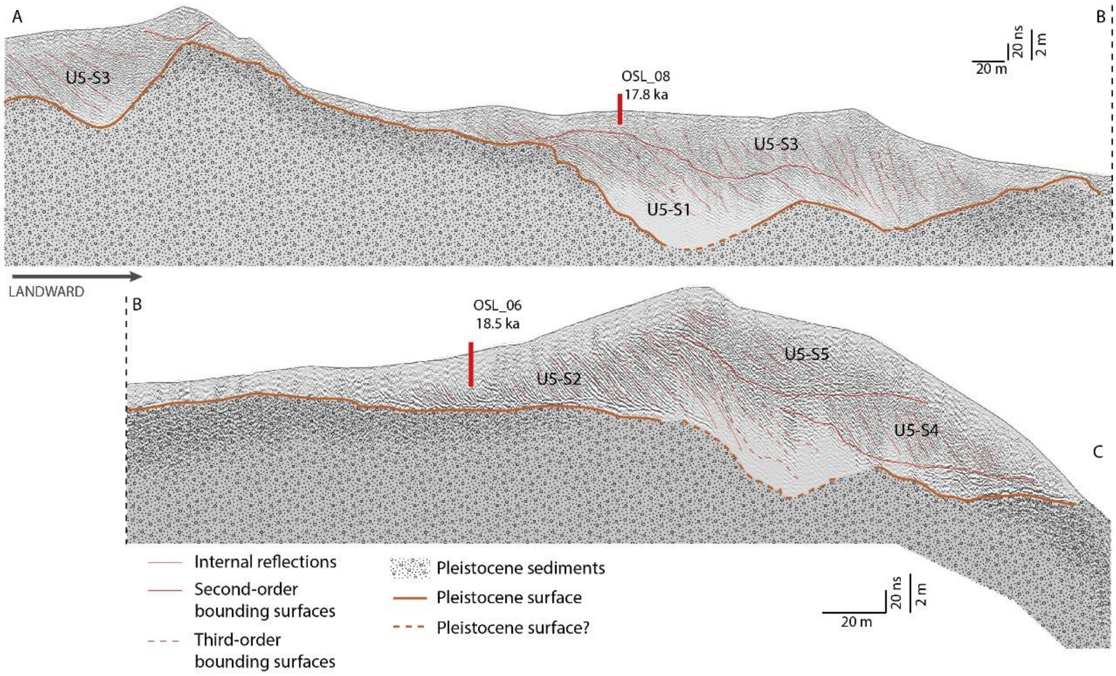

Figure 3. GPR line surveyed within the inland transgressive dunefield. For line location see Fig. 1.

The spatial distribution of the ages does not show a clear temporal segregation (Fig. 1); oldest dunes are partially covered and surrounded by younger dunes. The latter supports the eastward influx of aeolian sediment during different episodes of dune building rather than its continuous recycling. On the other hand, the large range of ages found in this area suggests that this terrace functioned as a trap to the aeolian sand migrating inland. Sand encroachment on this area could be explained by the morphology of the Pleistocene terrace, which gently dips landward, creating a shadow area with wind power reduction that could force the dunes to settle and stop their landward migration.

Following this extensive episode of aeolian activity, new pulses of sand drift during the Late- and Mid-Holocene suggest the onset of new major episodes of aeolian activity responsible for the formation of the cliff-top dune ridge (Costas et al., 2012). The stratigraphy of the cliff-top dune, combined with the analysis of its morphology from a digital terrain model, shows two vertically stacked units resulting from merged parabolic dunes advancing inland simultaneously (Costas et al., 2012). These are fixed once they reach the edge of the cliff to form the cliff-top ridge as they reach an area of flow separation just landward of the cliff. Stacking of units supports successive episodes of dune activity separated by periods of dune stabilization marked by the presence of a super-bounding surface (Costas et al., 2012). The latter marks the stabilization of the aeolian unit deposited 5.6 ka ago, during the Mid-Holocene, and the encroachment of a new sand unit during the Late-Holocene (1.20-0.98 ka). The last unit was reactivated between 0.44 and 0.30 ka, during the Little Ice Age (LIA). Finally, the dune ridge appears locally fragmented as a consequence of the isolation of individual parabolic dunes that continue their migration inland. This was the case of the aeolian unit dated at 0.15 ka (Fig. 1). Age determination of two subunits generated during the last reactivation of the dune between 0.44 and 0.30 ka, allowed estimating a migration rate of the dune during this period of time. The latter suggests that the dune was migrating at rates around 16.21 $m^3 m^{-1} yr^{-1}$ (i.e. 43000 kg $m^{-1} yr^{-1}$).

A major difference between the dunes within the cliff-top ridge and the inland coversand is the distances that they must have travelled before being fixed. If we assume that sediment is transferred inland through the migration of transgressive dunes fragmented from a former coastal barrier, the distance travelled by Late-Pleistocene dunes should range between 10 and 7 km while Holocene dunes should have migrated about 1 km. The longer transported distances occurred during the last termination when sea-level was lower but rising from about 120 to 50 m below MSL (Lambeck et al., 2014). Conversely, short distance Holocene transgressive dunes were formed after sea level reached its present position 7 ka ago (Vis et al., 2008).

4.2 Building present day analogs

This section explores the conditions for entrainment of past sand dunes and present day windfield regime to test the following hypothesis: present-day winds are not compatible with past aeolian activity because of a significant reduction of windiness (wind power per year) relative to windfield regimes responsible for major past events of aeolian activity.

4.2.1 Present-day windfield regime

The 10 years wind record of observations obtained from the present beach shows that the local windfield is dominated by winds approaching from north-northeast (18%) and north-northwest directions (19%) (Fig. 4A). About 41% of the record is represented by westerly winds (wind directions between 225 and 315º).

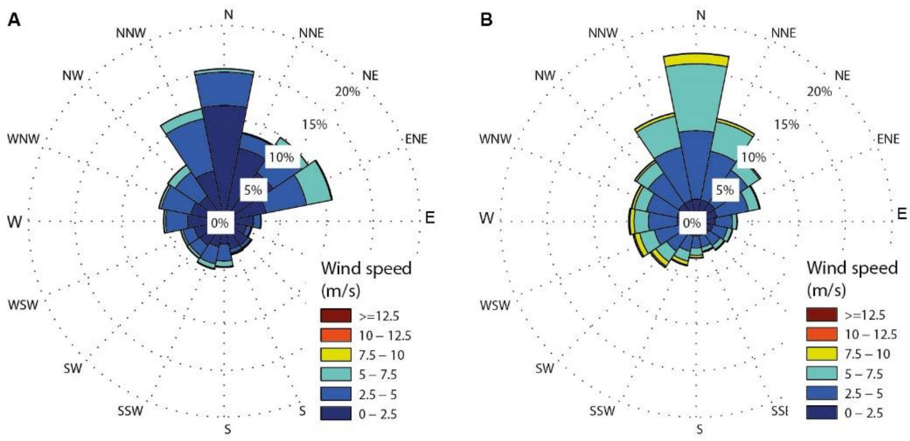

Figure 4. Wind rose of the 10 year record of local wind observations (A), and of the 49 years hindcast surface winds (B).

Frequent wind velocities are below 3 m s^{-1} (59%) while winds above 6 ms^{-1} constitute only 3% of the entire record (Fig. 4). Yet, most intense winds are blowing from the south-southwest when cyclones approach the Portuguese coast, contributing significantly to the resultant drift direction (RDP, Fig. 5) and to the low ratios of RDP/DP (Fig. 5A), which are in turn indicative of multidirectional winds.

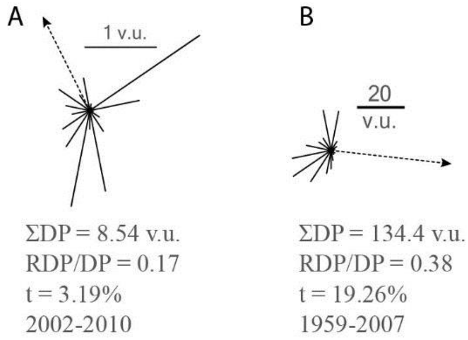

Figure 5. Sand rose showing local drift potential based on the 10 year record of local wind observations (A), and based on the 49 years of surface winds hindcast (B). The arrow shows the magnitude of the resultant drift potential (RDP, dashed line) and the resultant drift direction. *DP* represents the total drift potential, and *t* is the time the wind blew above the threshold velocity (in percent).

In an attempt to extend the wind record back in time, we examine a 49 years hindcast for the same location and compare with local observations using the same sampling interval for the period of time that both dataset overlap (Fig. 6). The comparison shows a good correspondence despite a weak correlation (R-square 0.30) and a systematic wind intensity overestimation of about 2 ms^{-1} (Fig. 6). Wind simulated directions indicate that northerly winds (north-northeast and north-northwest) are more frequent than observations, suggesting the influence of the local orography on shifting wind directions towards the west. The latter explains the higher contribution of southerly winds to RDP (Fig 5). Regarding wind intensities, simulated winds indicate that the area is dominated by winds below 7 ms^{-1} (83%).

Overall, the evaluation of present winds as potential transport agent suggests a low energy environment (DP< 200 VU) dominated by multidirectional winds (low to intermediate RDP/DP, Fig. 5). Potential sediment transport at the study area was estimated using the simulated winds because: (1) the dataset covers a longer period of time, and (2) it does not account for orographic or other surface roughness effects, which in turn may have changed over time, e.g. as shoreline migrated several kilometers eastward accompanying sea level rise.

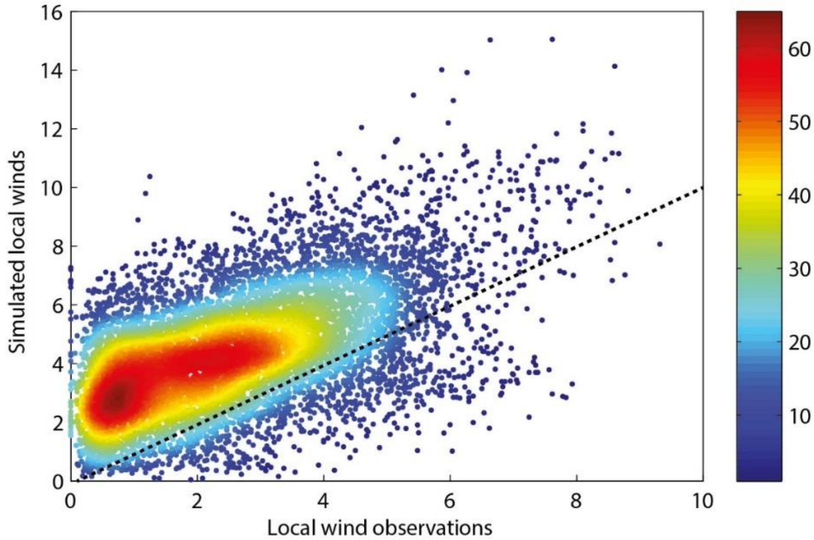

Figure 6. Scatter plot of local wind observations versus wind simulations for the same period of time and using the same sampling interval. Colours indicate data density.

4.2.2 Potential sediment transport

Textural analysis of samples representative of the transgressive dunefield indicate that the explored dunes consist of well-rounded and moderately well-sorted, coarse quartz sand (> 90% of SiO_2). Median-grain diameters ranged between 0.40 and 0.75 mm with negatively skewed grain size distributions (Table 1, Fig. 7), tailoring towards coarser sediments. Finer sediments were found within the Late Holocene units (Table 1, Fig. 7). Finally, modern dunes are conformed by finer sediments, symmetric and more leptokurtic (peaked) grain size distributions (Fig. 7). Grain size distributions suggest that Holocene sediments are a mix of the sediments within the last termination and the modern dunes.

Table 1. Sediment texture.

Age interval (ka)	Nº samples	Mean D_{50} (mm)	Maximum D_{50} (mm)	Minimum D_{50} (mm)
20-11.6	13	0.60	0.75	0.50
5.6-0.15	7	0.50	0.62	0.40
Modern	5	0.29	0.33	0.25

Threshold wind velocities estimated for the sediments conforming the transgressive dunes indicate critical velocities above 9.11 m s^{-1} and 9.84 m s^{-1} for the Late Holocene and last termination dunes respectively. Modern dune sediments indicate lower values with critical velocities around 7 m s^{-1}.

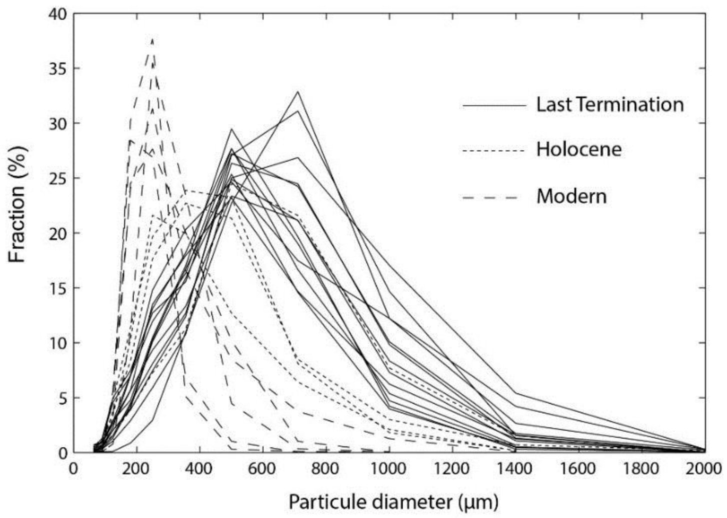

Figure 7. Grain size distribution of the analysed samples collected within the modern, the Late Holocene and last termination dunes.

Threshold velocities were contrasted with simulated winds to evaluate dune mobility under present windfield regimes. For that, we have filtered the data for different threshold wind velocities and favorable wind angle ranges (i.e. between 225 and 315º). Simulated winds suggest that threshold wind velocities for sand entrainment are rarely reached (Fig. 8A, B). Simulated westerly winds compatible with the migration of the Holocene transgressive dunes (i.e. 225-315º and wind speeds above 9.11 m s^{-1}) represented 0.83 % of the total number of records while winds compatible with modern dunes were recorded about 2.5 % of the record. Simulated winds compatible with the last termination dunes were recorded about 0.5 % of the time, explaining very low sediment transport potentials per year. Indeed, maximum sediment transport potentials compatible with the older dunes were estimated for the year 1966 (about 2500 kg m^{-1} yr^{-1}, Fig. 8C), and represent less than one order of magnitude of the sediment transport rates estimated for the LIA (i.e. 43000 kg m^{-1} yr^{-1}). Estimated transport potentials suggest that values above 2000 kg m^{-1} yr^{-1} are rare and have been only reached before the mid-80s. On the other hand, sediment transport potentials compatible with Late Holocene dunes may reach values of 3200 kg m^{-1} yr^{-1} (Fig. 8C) while estimates assuming present day dune sediments reach values of 5000 kg m^{-1} yr^{-1}, compatible with the small size of modern dunes.

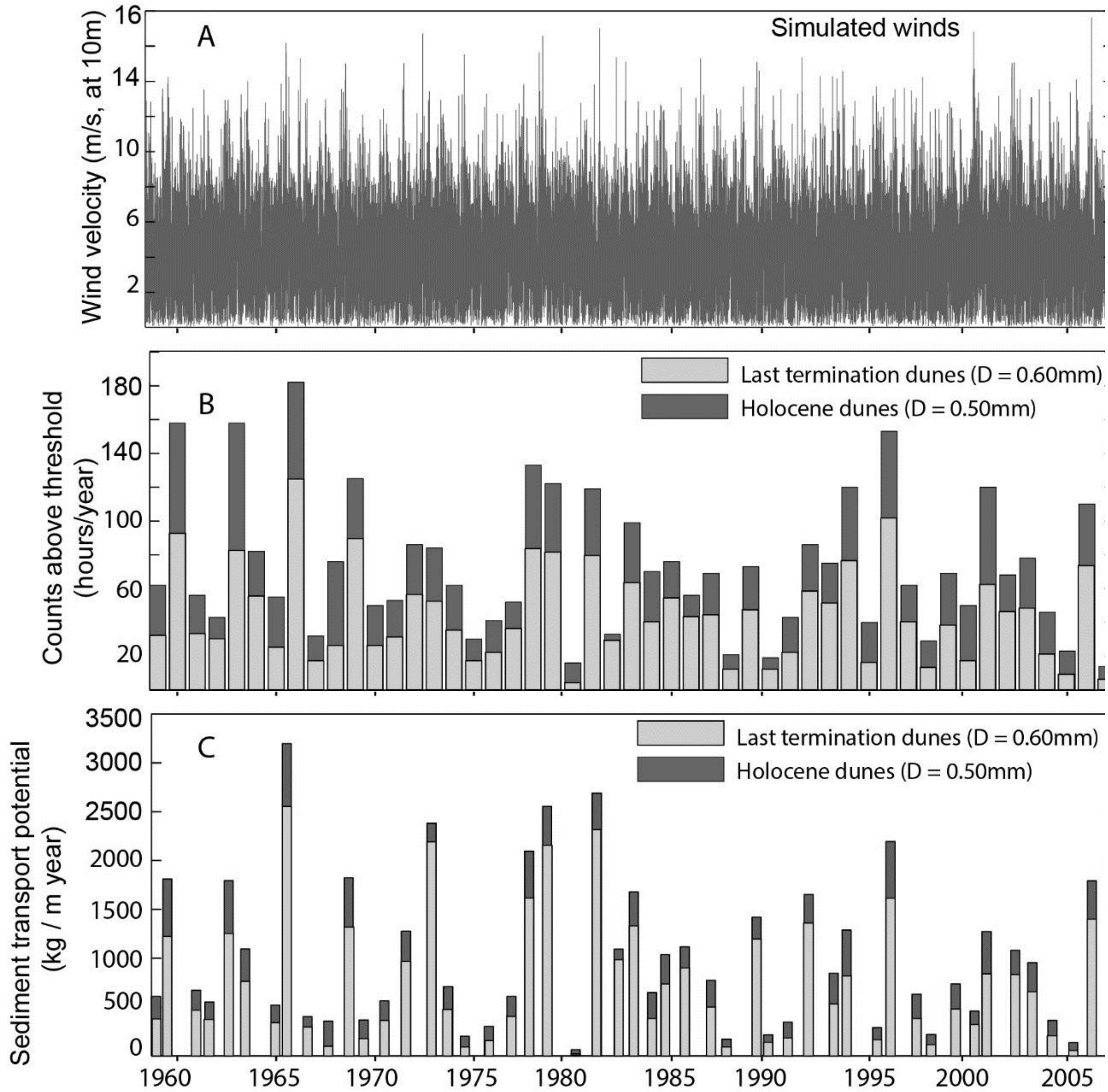

Figure 8. Estimation of the sediment transport potentials per year for the entire simulated dataset. (A) Simulated wind dataset, (B) number of hours or records per year with velocities above wind velocity threshold (i.e. 9.11 m s-1), and (C) estimated potential sediment transport per year.

Smaller grain sizes within the modern aeolian system suggest either a change in the sediment source over time, or less powerful winds and waves impacting the study area. Changes in the sediment supply are not easy as the most important source of sediments to the study area depends on the continuous recycling from in situ deposits such as the unconsolidated cliff (Costas et al., 2012). Conversely, finer sediments at the beach could be explained if wave energy is lowered while reduced wind speeds could explain finer grain sizes, the reduced scale of the dunes (maximum dune thickness around 3 meter), and its rapid vegetation colonization.

5. DISCUSSION

5.1 Atmospheric circulation

Present-day winds have been explored here to identify recent atmospheric circulation patterns compatible with aeolian activity in southern Europe through the Holocene and the last termination. For this, we have selected two representative events from local observations compatible with past aeolian activity (i.e. local wind velocities above threshold and events extending more than 60 min). Once the events were selected (27 February 2010 and 31 October 2003), the corresponding northeast Atlantic surface pressure maps were closely analyzed to find the main patterns susceptible to promoting intense westerly winds over the western Portuguese coast in the present-day climate (Fig. 9).

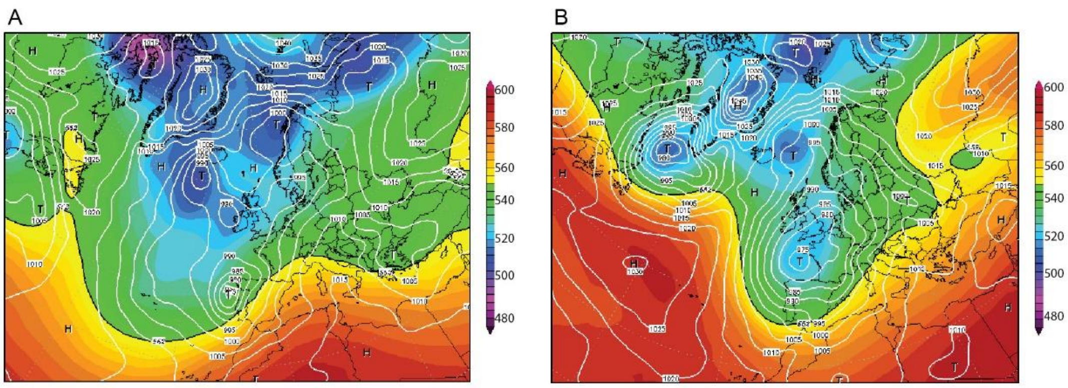

Figure 9. Surface pressure maps for the northeastern Atlantic region showing the patterns that promote the incidence of strong westerly winds over the western Portuguese coast. Contour lines represent surface pressure (in hPa) and the colour shading the 500 hPa geopotential height (in geopotential decametres, or gpdm) (source: www.wetterzentrale.de/).

The first is represented by surface pressure conditions showing several and fragmented low pressure systems along the Atlantic European coasts from the northern Scandinavia to the Iberian Peninsula, and relatively weak highs around Iceland (Fig. 9A). This pattern is compatible with a jet stream diverted to the south by the presence of high pressure blocking ridges in a context of weakened polar vortex. Under these conditions, windy events at the Portuguese coast result from the direct impact of cyclones following a southern track under conditions of persistent negative daily values of the NAO index. This pattern dominated the winter season of 2009/2010. A good example was the severe Xynthia windstorm that impacted western Europe in February 2010, claiming dozens of casualties and causing major damage along the Iberian Peninsula, France, Germany and the Benelux countries. During this event, the center of the low pressure approached the Iberian Peninsula coast following an unusual SW-NE path that generated very strong southerly winds (Vicente-Serrano et al., 2011).

The second pattern is characterized by the presence of very deep low pressure systems displaced to the south of Iceland and centered over the British Islands. These systems may extend their influence over the entire western coast of Europe, promoting strong westerly winds from northern Europe to Portugal (Fig. 9B). This pattern is also well represented by the conditions that prevailed during the 2013/2014 winter season over the western coast of Europe. As a consequence, very large floods occurred in the United Kingdom and France, while severe coastal damages took place in the Iberian Peninsula with dramatic consequences for local economies. Such conditions are characterized by positive, but relatively low values of the daily NAO index.

Both situations represent events during which westerly winds have enough power to promote aeolian sediment transport of medium to coarse sand as storms are enhanced at the end of a southward deflected NA storm track. It is worth noticing that both situations are favorable to the occurrence of “relative” blocking as the Icelandic Low is less deep (but not permanently replaced by an absolute high pressure cell as in “real” blocking). The mechanistic scenarios identified here support the study carried out by Raible et al. (2007), who found the southward shift of the cyclone storm track and a pronounced increase in extreme wind speeds south of 50º during the LIA triggered by a relatively strong cooling over the northernmost Atlantic. However, at present these rare events represent synoptic time scales of short duration (i.e. less 1.5 days) that contrast with more permanent negative conditions reproduced by proxies and simulations during the LIA (Baker et al., 2015; Trouet et al., 2012). Indeed, present-day analogs suggest that dunes sharing the features of the explored record would very unlikely form under present conditions because of the resultant low drift potentials and multidirectional winds. Indeed, the latter are not compatible with the formation of parabolic dunes as the observed within the aeolian record.

The two modern events provide a good indication of the conditions that were responsible for dune deposition during the last termination and the Holocene, setting atmospheric circulation patterns compatible with large-scale aeolian activity at southern Europe to more permanent low values of the NAO index. The latter implies the southward shift of the NA the storm track and the associated westerly winds. Indeed, Estimates of potential sediment transport show higher values during the first half of the explored dataset (Figure 8C), which is dominated by negative to relatively low values of the NAO index (Hurrell, 1995).

5.2 Major pulses of aeolian activity in the past

The extended and improved record of aeolian activity from the central coast of Portugal traces favorable conditions for dune building episodes in southern Europe over the last 20.5 ka centered at 0.35, 1.10, 5.60 and 17.5 ka (Fig. 2). The identified episodes suggest the southward deflection of the NA storm track and the strengthening of the westerlies over southern Europe during well-known climatic extremes such as the Heinrich event 1 (HE1) (Hemming, 2004), the 5.6 ka event (Mayewski et al., 2004), the end of the Dark Ages (Helama et al., 2009), and the LIA (Bradley and Jones, 1993).

5.2.1 The Holocene

The occurrence of discrete events of aeolian activity recorded through the Holocene suggests the onset of wind conditions enhancing aeolian activity during short periods of time. The record of aeolian activity represents periods of enhanced storminess (Costas et al., 2012), whose temporal distribution appears in phase with storminess periods affecting northern and central Europe (Orme et al., 2015; Sorrel et al., 2012; Trouet et al., 2012 and references therein). The synchronicity of these events is illustrated in Fig. 10, which compiles the spatial and temporal distribution of storminess periods during the Holocene based on: (i) aeolian activity related to dune mobility (Bateman and Godby, 2004; Clarke et al., 2002; Clemmensen et al., 2009; Costas et al., 2013; Gilbertson et al., 1999; Wilson et al., 2004), loess deposition (Jackson et al., 2005), clastic material concentration on raised bogs (Björck and Clemmensen, 2004; Jong et al., 2006; Orme et al., 2015), or chemical species in polar snow (Mayewski et al., 1997), (ii) occurrence of storm-related coastal deposits (Degeai et al., 2015; Sabatier et al., 2012; Sorrel et al., 2012; Van Vliet-Lanoë et al., 2014), and (iii) glacier evolution (Bakke et al., 2008). The observed distribution claims periods of enhanced storminess across Europe during the LIA, the end of the Dark Ages and during the Mid-Holocene, supporting a pattern that conflicts with the typical dipole configuration displayed by the NAO.

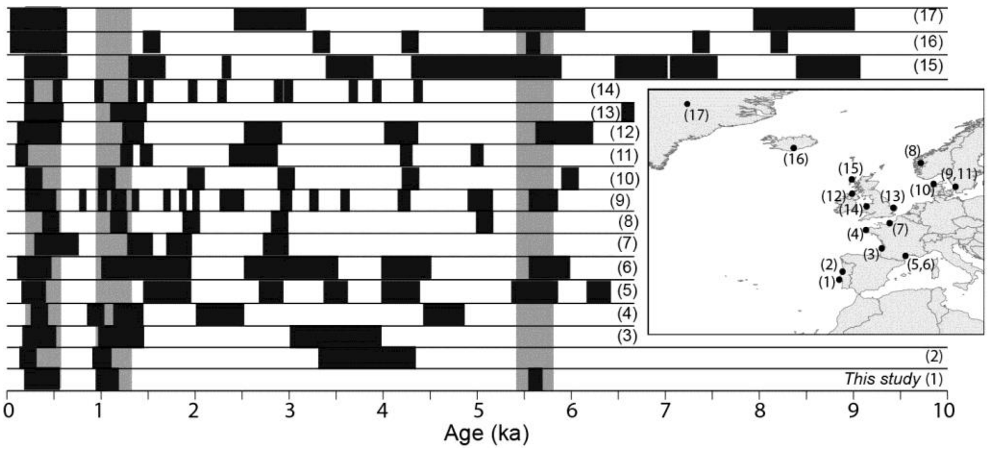

Figure 10. Temporal and spatial distribution of storminess periods over the Holocene (black boxes). The gray vertical bars represent the timing of the episodes identified within the present work and by Costas et al. (2012) over the Holocene. The numbers represent the different selected locations across Europe: 1 (this study), 2 (Costas et al., 2013), 3 (Clarke et al., 2002), 4 (Van Vliet-Lanoë et al., 2014), 5 (Sabatier et al., 2012), 6 (Degeai et al., 2015), 7 (Sorrel et al., 2012), 8 (Bakke et al., 2008), 9 (Björck and Clemmensen, 2004), 10 (Clemmensen et al., 2009), 11 (Jong et al., 2006), 12 (Wilson et al., 2004), 13 (Bateman and Godby, 2004), 14 (Orme et al., 2015), 15 (Gilbertson et al., 1999), 16 (Jackson et al., 2005), and 17 (Mayewski et al., 1997),.

The capability of the NAO of reconstructing past and historical climate conditions has been discussed due to inconsistencies in the relationship between the NAO and the proxy-based indices (Dawson et al., 2002). Indeed, it has been proven that the statistical relationship between proxy-based indices and the NAO is non-stationary, but it is highly dependent on the chosen verification periods (Schmutz et al., 2000), which may be characterized by different magnitudes of the variance between hemisphere parameters and the NAO (Schmutz et al., 2000). Indeed, the pattern of storminess distribution across Europe is compatible with the mechanistic scenarios proposed here and characterized by low to negative NAO in a context of Arctic amplification (i.e. the poles cooled more strongly than the Tropics). The latter can provoke changes to the centers of action of the NAO (Raible et al., 2006), and thus modify the expected relationship between proxy-based indicators and the NAO. Our results agree with Orme et al. (2015), who have found that periods of enhanced storminess at the UK could be compatible with low NAO within periods of frequent negative NAO.

5.2.2 The last termination

A major contribution of the present study is the extension of the record of aeolian activity back in time to the LGM, when boundary conditions were markedly different from the Holocene. During the LGM, a large portion of northern Eurasia and North America was covered by ice sheets with significant consequences on the albedo and over the large-scale atmospheric circulation in the Northern Hemisphere (Pausata et al., 2011).

The new ages support continuous aeolian activity between 20.5 ka ago and the late YD (11.6 ka) with a maximum around 17.5 ka, coincident with the HE1. These results suggest the southward migration of the NA jet stream, reaching the Iberian Peninsula, with a maximum impact of the westerlies during the peak of aeolian activity. Indeed, the larger mean grain sizes, spatial coverage and volume of sediment within the dunes built during the last termination relative to the dunes assigned to the Holocene (Fig. 1), together with the greater distances travelled by the former, support more intense winds during the last termination than during most of the Holocene period.

This scenario implies that substantial amounts of precipitation could be brought to the Iberian Peninsula by the westerlies, especially during winter (Cortesi et al., 2014). However, proxy-based reconstructions do not always agree with the proposed scenario, suggesting alternative scenarios ranging from humid to semi-arid conditions. Reconstructions based on lake levels and speleothems from the Iberian Peninsula document relatively humid conditions during the LGM (Moreno et al., 2012; Moreno et al., 2010). Lake indicators have been primarily linked to relatively humid conditions although alternative interpretations, including a reduction on evapotranspiration or increasing ice melting, have not been totally discarded (Moreno et al., 2012). Indeed, marine pollen sequences suggest overall dry and cold conditions between 27 ka and 15 ka (Fletcher and Sánchez Goñi, 2008). The latter is supported by very low precipitation levels documented by other lake and continental pollen sequences during the LGM (González-Sampériz et al., 2006; Morellón et al., 2009).

On the other hand, general circulation models consistently show a large scale picture dominated by the southward shift of a stronger, more zonally oriented NA jet stream (Beghin et al., 2015; Laîné et al., 2009; Li and Battisti, 2008; Pausata et al., 2011). Simulated patterns are forced by (i) steep meridional temperature gradients (Beghin et al., 2015; Laîné et al., 2009), and (ii) the ice sheet topography (Pausata et al., 2011). Interestingly, simulations suggest contrasting levels of precipitation. Laîné et al. (2009) simulated an amplification of the synoptic activity to the southeast, around the region between the Azores Islands and the Iberian peninsula while Li and Battisti (2008) performed a reduction of the wintertime eddy activity at all levels of the atmosphere. These results are supported by our records, as in both cases the southward shift of the jet stream and associated westerlies are simulated. However, the ambiguity related to the levels of precipitation remains open. Beghin et al. (2015) found that inconsistences between proxies could result from contrasting seasonal changes in precipitation (i.e. wet winters and dry summers). Indeed, the authors found that the amount of winter precipitation correlates with to the southward latitudinal shift of the jet. If so, the record of aeolian activity, which has been proven to trace the impact of the NA westerly winds, could contribute to reconstruct not only dominant winds but also precipitation. If so, could we assume that higher precipitation should be expected during the HE1?

Most of the existent climate reconstructions based on paleo-climate archives agree to associate the HE1 to drier and colder conditions (Fletcher and Sánchez Goñi, 2008;

Moreno et al., 2012; Moreno et al., 2010), with maximum aridity assigned to 17.5 ka (Moreno et al., 2010). Despite this apparent consensus, Naughton et al. (2009) documented colder and wetter conditions during a first phase of the HE1, which was followed by more arid conditions after 17.5 ka, coincident with the reduction of aeolian activity. Model simulations suggest the maintenance of the jet stream at lower latitudes (Roberts et al., 2014). However, uncertainties related to the relative levels of precipitation in southern Europe are elevated as it is highly dependent on the sea surface temperature (Kageyama et al., 2005).

Following the peak of maximum activity at 17.5, aeolian activity gradually diminished, showing an apparent stop around 14 ka. This trend suggests a concomitant reduction of the strength of the westerlies along the Portuguese coast and the northward shift of the storm track. Simultaneously, warmer conditions advanced across the Iberian Peninsula leading to rapid forest expansion (Fletcher and Sánchez Goñi, 2008). These environmental responses agree with simulations obtained by Renssen and Bogaart (2003), which suggest the northward relocation of the jet after 14.7 ka with the northward retreat of the sea ice.

Aeolian activity, although probably more intermittently, continued until the end of the YD, suggesting the intermittent or less profound visit of the NA westerlies to the Iberian Peninsula. Indeed, proxy-based reconstructions and model simulations suggest the re-advance of sea ice during the YD, promoting the southward shift of the westerlies (Bakke et al., 2009). The YD is documented as a rather complex event with a first phase characterized by dry and cold atmospheric conditions according to marine pollen sequences from southern Iberia (Fletcher and Sánchez Goñi, 2008). This first phase was followed by a relative increase in precipitation after 12.5 ka recorded by speleothems and marine pollen sequences (Bartolomé et al., 2015; Fletcher and Sánchez Goñi, 2008). Conversely, Baldini et al. (2015) found an additional and more humid phase between 12.5 and 12.15 ka using speleothems from northern Iberia, suggesting the southward shift of the westerlies and the subsequent northward relocation after 12.15 ka. Interestingly, a parallel pattern was documented in northern Europe despite a slight delay on the response (Lane et al., 2013). The YD in northern Europe was characterized by an initial cold phase followed by a second phase of climatic amelioration related to a northward shift of the westerly wind systems (Lane et al., 2013).

The above supports the hypothesis that the record of aeolian activity can successfully trace the southward migration of the NA westerly winds. Indeed, the meridional shifts of the jet stream and associated westerlies resemble the leading mode of variability in the instrumental record (i.e. the NAO), and thus the mechanistic scenarios found in section 5.1. However, the sustained episode of aeolian activity through the last termination supports relatively stationary atmospheric circulation regime dominated by strong and zonal westerly winds whose maximum southward excursion occurred 17.5 ka ago. Contrasting boundary conditions (i.e. volume of ice sheets and greenhouse gases) during the last termination could modify the configuration and variability of this NAO-like mode (Pausata et al., 2009). For instance, model simulations provide evidence for an altered atmospheric circulation regime under glacial conditions characterized by a stronger, more zonally oriented Atlantic jet but reduced storminess (Li and Battisti, 2008), and less interannual variability (Pausata et al., 2009) as supported by the aeolian record presented here. The latter suggests, that enhanced westerly winds over the Iberian Peninsula do not necessarily represent higher precipitation. Indeed, comparison with other indicators underlines the limitations of our record, which is a direct indicator of wind strength and direction, but it does not retain information about the amount of precipitation that those winds may have brought to the Iberian Peninsula. Yet, it is worth noticing that the type of dunes identified within the aeolian record (i.e. parabolic dunes) suggests that past dune migration should be dominated by unidirectional winds, relatively abundant vegetation and/or high water table levels.

6. CONCLUSIONS

From both our dunefield dataset and present-day wind analogs we can state that in the period between 20 ka and 0.15 ka four events of enhanced aeolian activity have occurred in Southern Europe due to exceptional intensifications of westerly winds visiting the Portuguese coast for sustained periods of time. Identified episodes of aeolian activity have been related here to the equatorward shift of the storm track forced by (1) the migration of the polar front in the same direction, promoting zonal circulation patterns in a context of glacial and transitional conditions, and (2) the onset of high pressures promoting relative blocking of cyclones in northern Europe and intense and sustained westerly winds and storms in southern Europe under interstadial conditions in a context of relative cooling (Artic amplification) over northernmost Atlantic.

Present-day analogs also suggest that dunes sharing the features of the aeolian record attributed to the last termination and the Holocene would very unlikely form under present conditions as they explain the migration of past dunes at much lower rates. In the case of the Caparica transgressive dunefield explored here, Costas et al. (2012) hypothesized the formation of the aeolian system linked to episodic enhanced westerly winds over a retreating former shoreline. The results presented here prove that recent (last 50 years) windfield regimes are incompatible with the landforms observed in the explored aeolian record, but with the smaller scale sedimentation observed nowadays within the present foredune with low sedimentation and mobilization rates. The latter supports the previous hypothesis and proposes that past aeolian activity could only have occurred if windiness (i.e. wind power and its duration over the year) increased along southwestern Europe in combination with high sediment availability.

ACKNOWLEDGMENTS

This research was founded by the Portuguese Science Foundation (FCT) through the projects SCARPS (PTDC/CTE-GIX/101466/2008). The first author was founded through the “FCT Investigator” program (ref. IF/01047/2014) and a research grant within the EU FP7 research project RISC-KIT-GA-2013-603458. Thanks are given to all the people that helped during the fieldwork and with fruitful discussions during the entire process. The authors also want to thank Sonia Jerez for providing the wind data simulations. Finally, the authors would like to thank the three reviewers whose comments and suggestions contributed to improve the manuscript significantly.

REFERENCE LIST

Bagnold, R.A., 1941. The Physics of Blown Sand and Desert Dunes. Methuen, London.

Baker, A., C. Hellstrom, J., Kelly, B.F.J., Mariethoz, G., Trouet, V., 2015. A composite annual-resolution stalagmite record of North Atlantic climate over the last three millennia. Sci. Rep. 5.

Bakke, J., Lie, Ø., Dahl, S.O., Nesje, A., Bjune, A.E., 2008. Strength and spatial patterns of the Holocene wintertime westerlies in the NE Atlantic region. Global and Planetary Change 60, 28-41.

Bakke, J., Lie, O., Heegaard, E., Dokken, T., Haug, G.H., Birks, H.H., Dulski, P., Nilsen, T., 2009. Rapid oceanic and atmospheric changes during the Younger Dryas cold period. Nature Geosci 2, 202-205.

Baldini, L.M., McDermott, F., Baldini, J.U.L., Arias, P., Cueto, M., Fairchild, I.J., Hoffmann, D.L., Mattey, D.P., Müller, W., Nita, D.C., Ontañón, R., Garciá-Moncó, C., Richards, D.A., 2015. Regional temperature, atmospheric circulation, and sea-ice variability within the Younger Dryas Event constrained using a speleothem from northern Iberia. Earth and Planetary Science Letters 419, 101-110.

Bartolomé, M., Moreno, A., Sancho, C., Stoll, H.M., Cacho, I., Spötl, C., Belmonte, Á., Edwards, R.L., Cheng, H., Hellstrom, J.C., 2015. Hydrological change in Southern Europe responding to increasing North Atlantic overturning during Greenland Stadial 1. Proceedings of the National Academy of Sciences 112, 6568-6572.

Bateman, M.D., Godby, S.P., 2004. Late-Holocene inland dune activity in the UK: a case study from Breckland, East Anglia. The Holocene 14, 579-588.

Beghin, P., Charbit, S., Kageyama, M., Combourieu-Nebout, N., Hatté, C., Dumas, C., Peterschmitt, J.Y., 2015. What drives LGM precipitation over the western Mediterranean? A study focused on the Iberian Peninsula and northern Morocco. Climate Dynamics, 1-21.

Björck, S., Clemmensen, L.B., 2004. Aeolian sediment in raised bog deposits, Halland, SW Sweden: a new proxy record of Holocene winter storminess variation in southern Scandinavia? The Holocene 14, 677-688.

Björck, S., Walker, M.J.C., Cwynar, L.C., Johnsen, S., Knudsen, K.-L., Lowe, J.J., Wohlfarth, B., 1998. An event stratigraphy for the Last Termination in the North Atlantic region based on the Greenland ice-core record: a proposal by the INTIMATE group. Journal of Quaternary Science 13, 283-292.

Bradley, R.S., Jones, P.D., 1993. 'Little Ice Age' summer temperature variations: their nature and relevance to recent global warming trends. The Holocene 3, 367–376.

Chase, B., 2009. Evaluating the use of dune sediments as a proxy for palaeo-aridity: A southern African case study. Earth-Science Reviews 93, 31-45.

Clarke, M., Rendell, H., Tastet, J.-P., Clave, B., Masse, L., 2002. Late-Holocene sand invasion and North Atlantic storminess along the Aquitaine Coast, southwest France. The Holocene 12, 231-238.

Clemmensen, L.B., Murray, A., Heinemeier, J., de Jong, R., 2009. The evolution of Holocene coastal dunefields, Jutland, Denmark: A record of climate change over the past 5000 years. Geomorphology 105, 303-313.

Cortesi, N., Gonzalez-Hidalgo, J.C., Trigo, R.M., Ramos, A.M., 2014. Weather types and spatial variability of precipitation in the Iberian Peninsula. International Journal of Climatology 34, 2661-2677.

Costas, S., Brito, P., Fitzgerald, D., Goble, R., 2013. Climate-driven episodes of dune mobilization and barrier growth along the central coast of Portugal. Geological Society, London, Special Publications 388.

Costas, S., Jerez, S., Trigo, R.M., Goble, R., Rebêlo, L., 2012. Sand invasion along the Portuguese coast forced by westerly shifts during cold climate events. Quaternary Science Reviews 42, 15–28.

Dawson, A.G., Hickey, K., Holt, T., Elliott, L., Dawson, S., Foster, I.D.L., Wadhams, P., Jonsdottir, I., Wilkinson, J., McKenna, J., Davis, N.R., Smith, D.E., 2002. Complex North Atlantic Oscillation (NAO) Index signal of historic North Atlantic storm-track changes. The Holocene 12, 363-369.

Degeai, J.-P., Devillers, B., Dezileau, L., Oueslati, H., Bony, G., 2015. Major storm periods and climate forcing in the Western Mediterranean during the Late Holocene. Quaternary Science Reviews 129, 37-56.

Fletcher, W.J., Sánchez Goñi, M.F., 2008. Orbital- and sub-orbital-scale climate impacts on vegetation of the western Mediterranean basin over the last 48,000 yr. Quaternary Research 70, 451-464.

Fryberger, S.G., 1979. Dune forms and wind regime, by Steven G. Fryberger, assisted by Gary Dean, in: McKee, E.D. (Ed.), A study of global sand seas. U. S. Geological Survey, Reston, Virginia, pp. 137-170.

Galbraith, R.F., Roberts, R.G., Laslett, G.M., Yoshida, H., Olley, J.M., 1999. Optical dating of single and multiple grains of quartz from Jinmium Rock Shelter, Northern Australia: Part I, experimental design and statistical models. Archaeometry 41, 339–364.

Gilbertson, D.D., Schwenninger, J.L., Kemp, R.A., Rhodes, E.J., 1999. Sand-drift and Soil Formation Along an Exposed North Atlantic Coastline: 14,000 Years of Diverse Geomorphological, Climatic and Human Impacts. Journal of Archaeological Science 26, 439-469.

González-Sampériz, P., Valero-Garcés, B.L., Moreno, A., Jalut, G., García-Ruiz, J.M., Martí-Bono, C., Delgado-Huertas, A., Navas, A., Otto, T., Dedoubat, J.J., 2006. Climate variability in the Spanish Pyrenees during the last 30,000 yr revealed by the El Portalet sequence. Quaternary Research 66, 38-52.

Helama, S., Meriläinen, J., Tuomenvirta, H., 2009. Multicentennial megadrought in northern Europe coincided with a global El Niño–Southern Oscillation drought pattern during the Medieval Climate Anomaly. Geology 37, 175-178.

Hemming, S.R., 2004. Heinrich events: Massive late Pleistocene detritus layers of the North Atlantic and their global climate imprint. Rev. Geophys. 42, RG1005.

Hurrell, J.W., 1995. Decadal Trends in the North Atlantic Oscillation: Regional Temperatures and Precipitation. Science 269, 676-679.

Jackson, M.G., Oskarsson, N., Trønnes, R.G., McManus, J.F., Oppo, D.W., Grönvold, K., Hart, S.R., Sachs, J.P., 2005. Holocene loess deposition in Iceland: Evidence for millennial-scale atmosphere-ocean coupling in the North Atlantic. Geology 33, 509-512.

Jerez, S., Trigo, R.M., Vicente-Serrano, S.M., Pozo-Vázquez, D., Lorente-Plazas, R., Lorenzo-Lacruz, J., Santos-Alamillos, F., Montávez, J.P., 2013. The Impact of the North Atlantic Oscillation on Renewable Energy Resources in Southwestern Europe. Journal of Applied Meteorology and Climatology 52, 2204-2225.

Jong, R.d., Björck, S., Björkman, L., Clemmensen, L.B., 2006. Storminess variation during the last 6500 years as reconstructed from an ombrotrophic peat bog in Halland, southwest Sweden. Journal of Quaternary Science 21, 905-919.

Kageyama, M., Nebout, N.C., Sepulchre, P., Peyron, O., Krinner, G., Ramstein, G., Cazet, J.-P., 2005. The Last Glacial Maximum and Heinrich Event 1 in terms of climate and vegetation around the Alboran Sea: a preliminary model-data comparison. Comptes Rendus Geoscience 337, 983-992.

Laîné, A., Kageyama, M., Salas-Mélia, D., Voldoire, A., Rivière, G., Ramstein, G., Planton, S., Tyteca, S., Peterschmitt, J.Y., 2009. Northern hemisphere storm tracks during the last glacial maximum in the PMIP2 ocean-atmosphere coupled models: energetic study, seasonal cycle, precipitation. Climate Dynamics 32, 593-614.

Lambeck, K., Rouby, H., Purcell, A., Sun, Y., Sambridge, M., 2014. Sea level and global ice volumes from the Last Glacial Maximum to the Holocene. Proceedings of the National Academy of Sciences 111, 15296-15303.

Lancaster, N., 1981. Paleoenvironmental implications of fixed dune systems in Southern Africa. Palaeogeography, Palaeoclimatology, Palaeoecology 33, 327-346.

Lancaster, N., Kocurek, G., Singhvi, A., Pandey, V., Deynoux, M., Ghienne, J.-F., Lô, K., 2002. Late Pleistocene and Holocene dune activity and wind regimes in the western Sahara Desert of Mauritania. Geology 30, 991-994.

Lane, C.S., Brauer, A., Blockley, S.P.E., Dulski, P., 2013. Volcanic ash reveals time-transgressive abrupt climate change during the Younger Dryas. Geology.

Lettau, K., Lettau, H., 1977. Experimental and Micrometeorological Field Studies of Dune Migration, in: Lettau, K., Lettau, H. (Eds.), Exploring the World's Driest Climate. University of Wisconsin Press, Madison, pp. 110-147.

Li, C., Battisti, D.S., 2008. Reduced Atlantic Storminess during Last Glacial Maximum: Evidence from a Coupled Climate Model. Journal of Climate 21, 3561-3579.

Lima, M.I.P.d., Marques, A.C., Lima, J.L.M.P.d., 2005. Análise de tendência da precipitação anual e mensal no período 1900-2000, em Portugal Continental. Territorium 12.

Lorente-Plazas, R., Montávez, J.P., Jerez, S., Gómez-Navarro, J.J., Jiménez-Guerrero, P., Jiménez, P.A., 2014. A 49 year hindcast of surface winds over the Iberian Peninsula. International Journal of Climatology, n/a-n/a.

Mayewski, P.A., Meeker, L.D., Twickler, M.S., Whitlow, S., Yang, Q., Lyons, W.B., Prentice, M., 1997. Major features and forcing of high-latitude northern hemisphere atmospheric circulation using a 110,000-year-long glaciochemical series. J. Geophys. Res. 102, 26345-26366.

Mayewski, P.A., Rohling, E.E., Curt Stager, J., Karlén, W., Maasch, K.A., David Meeker, L., Meyerson, E.A., Gasse, F., van Kreveld, S., Holmgren, K., Lee-Thorp, J., Rosqvist, G., Rack, F., Staubwasser, M., Schneider, R.R., Steig, E.J., 2004. Holocene climate variability. Quaternary Research 62, 243-255.

Morellón, M., Valero-Garcés, B., Vegas-Vilarrúbia, T., González-Sampériz, P., Romero, Ó., Delgado-Huertas, A., Mata, P., Moreno, A., Rico, M., Corella, J.P., 2009. Lateglacial and

Holocene palaeohydrology in the western Mediterranean region: The Lake Estanya record (NE Spain). Quaternary Science Reviews 28, 2582-2599.
Moreno, A., González-Sampériz, P., Morellón, M., Valero-Garcés, B.L., Fletcher, W.J., 2012. Northern Iberian abrupt climate change dynamics during the last glacial cycle: A view from lacustrine sediments. Quaternary Science Reviews 36, 139-153.
Moreno, A., Stoll, H., Jiménez-Sánchez, M., Cacho, I., Valero-Garcés, B., Ito, E., Edwards, R.L., 2010. A speleothem record of glacial (25–11.6 kyr BP) rapid climatic changes from northern Iberian Peninsula. Global and Planetary Change 71, 218-231.
Murray, A.S., Wintle, A.G., 2000. Luminescence dating of quartz using an improved single-aliquot regenerative-dose protocol. Radiation Measurements 32, 57–73.
Naughton, F., Sánchez Goñi, M.F., Kageyama, M., Bard, E., Duprat, J., Cortijo, E., Desprat, S., Malaizé, B., Joly, C., Rostek, F., Turon, J.L., 2009. Wet to dry climatic trend in north-western Iberia within Heinrich events. Earth and Planetary Science Letters 284, 329-342.
Orme, L.C., Davies, S.J., Duller, G.A.T., 2015. Reconstructed centennial variability of Late Holocene storminess from Cors Fochno, Wales, UK. Journal of Quaternary Science 30, 478-488.
Pausata, F.S.R., Li, C., Wettstein, J.J., Kageyama, M., Nisancioglu, K.H., 2011. The key role of topography in altering North Atlantic atmospheric circulation during the last glacial period. Clim. Past 7, 1089-1101.
Pausata, F.S.R., Li, C., Wettstein, J.J., Nisancioglu, K.H., Battisti, D.S., 2009. Changes in atmospheric variability in a glacial climate and the impacts on proxy data: a model intercomparison. Clim. Past 5, 489-502.
Raible, C., Casty, C., Luterbacher, J., Pauling, A., Esper, J., Frank, D., Büntgen, U., Roesch, A., Tschuck, P., Wild, M., Vidale, P.-L., Schär, C., Wanner, H., 2006. Climate variability — observations, reconstructions, and model simulations for the Atlantic-European and Alpine region from 1500–2100 AD, in: Wanner, H., Grosjean, M., Röthlisberger, R., Xoplaki, E. (Eds.), Climate Variability, Predictability and Climate Risks. Springer Netherlands, pp. 9-29.
Raible, C., Yoshimori, M., Stocker, T., Casty, C., 2007. Extreme midlatitude cyclones and their implications for precipitation and wind speed extremes in simulations of the Maunder Minimum versus present day conditions. Climate Dynamics 28, 409-423.
Renssen, H., Bogaart, P., 2003. Atmospheric variability over the ∼14.7 kyr BP stadial-interstadial transition in the North Atlantic region as simulated by an AGCM. Climate Dynamics 20, 301-313.
Roberts, W.H.G., Valdes, P.J., Payne, A.J., 2014. Topography's crucial role in Heinrich Events. Proceedings of the National Academy of Sciences of the United States of America 111, 16688-16693.
Sabatier, P., Dezileau, L., Colin, C., Briqueu, L., Bouchette, F., Martinez, P., Siani, G., Raynal, O., Von Grafenstein, U., 2012. 7000 years of paleostorm activity in the NW Mediterranean Sea in response to Holocene climate events. Quaternary Research 77, 1–11.
Schmutz, C., Luterbacher, J., Gyalistras, D., Xoplaki, E., Wanner, H., 2000. Can we trust proxy-based NAO index reconstructions? Geophysical Research Letters 27, 1135-1138.
Seager, R., Liu, H., Henderson, N., Simpson, I., Kelley, C., Shaw, T., Kushnir, Y., Ting, M., 2014. Causes of Increasing Aridification of the Mediterranean Region in Response to Rising Greenhouse Gases. Journal of Climate 27, 4655-4676.
Sorrel, P., Debret, M., Billeaud, I., Jaccard, S.L., McManus, J.F., Tessier, B., 2012. Persistent non-solar forcing of Holocene storm dynamics in coastal sedimentary archives. Nature Geoscience 5, 892–896.
Trouet, V., Esper, J., Graham, N.E., Baker, A., Scourse, J.D., Frank, D.C., 2009. Persistent Positive North Atlantic Oscillation Mode Dominated the Medieval Climate Anomaly. Science 324, 78–80.
Trouet, V., Scourse, J.D., Raible, C.C., 2012. North Atlantic storminess and Atlantic Meridional Overturning Circulation during the last Millennium: Reconciling contradictory proxy records of NAO variability. Global and Planetary Change 84–85, 48-55.

Tsoar, H., 2005. Sand dunes mobility and stability in relation to climate. Physica A: Statistical Mechanics and its Applications 357, 50-56.
Ulbrich, U., Lionello, P., Belušić, D., Jacobeit, J., Knippertz, P., Kuglitsch, F.G., Leckebusch, G.C., Luterbacher, J., Maugeri, M., Maheras, P., Nissen, K.M., Pavan, V., Pinto, J.G., Saaroni, H., Seubert, S., Toreti, A., Xoplaki, E., Ziv, B., 2012. 5 - Climate of the Mediterranean: Synoptic Patterns, Temperature, Precipitation, Winds, and Their Extremes, in: Lionello, P. (Ed.), The Climate of the Mediterranean Region. Elsevier, Oxford, pp. 301-346.
Van Vliet-Lanoë, B., Goslin, J., Hallégouët, B., Hénaff, A., Delacourt, C., Fernane, A., Franzetti, M., Le Cornec, E., Le Roy, P., Penaud, A., 2014. Middle- to late-Holocene storminess in Brittany (NW France): Part I – morphological impact and stratigraphical record. The Holocene 24, 413-433.
Vicente-Serrano, S., Trigo, R., López-Moreno, J.I., Liberato, M.L.R., Lorenzo-Lacruz, J., Beguería, S., Morán-Tejeda, E., Kenawy, A.E., 2011. Extreme winter precipitation in the Iberian Peninsula in 2010: anomalies, driving mechanisms and future projections. Climate Research 46, 51-65.
Vis, G.-J., Kasse, C., Vandenberghe, J., 2008. Late Pleistocene and Holocene palaeogeography of the Lower Tagus Valley (Portugal): effects of relative sea level, valley morphology and sediment supply. Quaternary Science Reviews 27, 1682–1709.
Wilson, P., McGourty, J., Bateman, M.D., 2004. Mid-to late-Holocene coastal dune event stratigraphy for the north coast of Northern Ireland. The Holocene 14, 406-416.